RESEARCH ARTICLE

# P2X7 activation enhances skeletal muscle metabolism and regeneration in SOD1G93A mouse model of amyotrophic lateral sclerosis

Paola Fabbrizio[1]; Savina Apolloni[2]; Andrea Bianchi[2]; Illari Salvatori[2]; Cristiana Valle[2,3];
Chiara Lanzuolo[2,4]; Caterina Bendotti[1]; Giovanni Nardo[1,*] (iD) ; Cinzia Volonté[2,5,*] (iD)

[1] Laboratory of Molecular Neurobiology, Department of Neuroscience, Istituto di Ricerche Farmacologiche Mario Negri IRCCS, Milan, Italy.

[2] IRCCS Fondazione Santa Lucia, Rome, Italy.

[3] National Research Council, Institute of Translational Pharmacology, Rome, Italy.

[4] National Research Council, Institute of Biomedical Technologies, Milan, Italy.

[5] National Research Council, Institute for Systems Analysis and Computer Science, Rome, Italy.

**Corresponding author:**

Giovanni Nardo, Laboratory of Molecular Neurobiology, Department of Neuroscience, Istituto di Ricerche Farmacologiche Mario Negri IRCCS, Via Mario Negri 2, 20156 Milan, Italy (E-mail: *giovanni.nardo@marionegri.it*)

Cinzia Volonté, National Research Council, Institute for Systems Analysis and Computer Science, Via dei Taurini 19, 00185 Rome, Italy (E-mail: *cinzia.volonte@cnr.it*)

*Co-last authors.

## Abstract

Muscle weakness plays an important role in neuromuscular disorders comprising amyotrophic lateral sclerosis (ALS). However, it is not established whether muscle denervation originates from the motor neurons, the muscles or more likely both. Previous studies have shown that the expression of the SOD1G93A mutation in skeletal muscles causes denervation of the neuromuscular junctions, inability to regenerate and consequent atrophy, all clear symptoms of ALS. In this work, we used SOD1G93A mice, a model that best mimics some pathological features of both familial and sporadic ALS, and we investigated some biological effects induced by the activation of the P2X7 receptor in the skeletal muscles. The P2X7, belonging to the ionotropic family of purinergic receptors for extracellular ATP, is abundantly expressed in the healthy skeletal muscles, where it controls cell duplication, differentiation, regeneration or death. In particular, we evaluated whether an *in vivo* treatment in SOD1G93A mice with the P2X7 specific agonist 2′(3′)-O-(4-Benzoylbenzoyl) adenosine5′-triphosphate (BzATP) just before the onset of a pathological neuromuscular phenotype could exert beneficial effects in the skeletal muscles. Our findings indicate that stimulation of P2X7 improves the innervation and metabolism of myofibers, moreover elicits the proliferation/differentiation of satellite cells, thus preventing the denervation atrophy of skeletal muscles in SOD1G93A mice. Overall, this study suggests that a P2X7-targeted and site-specific modulation might be a strategy to interfere with the complex multifactorial and multisystem nature of ALS.

## INTRODUCTION

Amyotrophic lateral sclerosis (ALS) is one of the most common neuromuscular disorders characterized by the selective loss of upper motor neurons in motor cortex, and lower motor neurons in the brainstem and spinal cord, accompanied by skeletal muscle atrophy and paralysis. The disease affects individuals from all ethnic backgrounds, with an incidence of 2–3 cases per 100.000 individuals per year (47). About 90% of all ALS cases is sporadic while the remaining 10% is of genetic origin. One form of familial ALS is caused by missense mutations in the gene encoding

the Cu/Zn superoxide dismutase enzyme (SOD1), which induces a gain of toxic function (8). This mutation is currently expressed in the animal model that best mimics some phenotypic and pathological feature of both familial and sporadic ALS, the SOD1G93A mouse (29).

It was reported that muscle weakness has an important role in ALS pathology, although it is not clear whether denervation originates from the motor neuron soma, or the muscle (27). Previous studies have shown that the exclusive expression of mutant SOD1G93A (mSOD1) in the skeletal muscles can lead to denervation of the neuromuscular junctions (NMJs), which lose the ability to

regenerate and become atrophic, thus contributing to the symptoms of ALS (7). Indeed, several mechanisms implicated in the physiological maintenance of skeletal muscle are deregulated in ALS, such as satellite cell (SC) activity, mitochondrial and miRNA biogenesis (17, 18, 31, 41). It is interesting that these processes act synergistically to maintain healthy skeletal muscle, and influence both the number and the activity of the innervated junctions (37).

The purinergic receptors, including the ionotropic P2X7 subtype, are expressed in skeletal muscles where they influence cell growth, differentiation, regeneration and death in health and disease (50). Several data suggest that P2X7 plays a beneficial role in the peripheral nervous system (PNS). For instance, P2X7 activation mediates Schwann cell proliferation after sciatic nerve injury (33), promotes myogenesis and the formation/function of NMJs (49).

We have previously shown that genetic ablation of P2X7 anticipates the disease onset and worsens the disease progression of mSOD1 mice (2). Conversely, the pharmacological systemic inhibition of P2X7 from late pre-onset of disease exerts a positive outcome on motor performance (3), and a slight beneficial effect on the survival of mSOD1 mice (5). This suggested a dual role played by P2X7 in modulating some pathological mechanisms of ALS. Further confirming this hypothesis, the *in vitro* activation of P2X7 by the agonist BzATP in mSOD1 mice-derived primary microglia elicits either M1 or M2 phenotypes depending on the persistence of activation. Moreover, the decrease of the autophagic marker SQSTM1/p62 can be obtained either in mSOD1 microglia by stimulating the P2X7 for a short time, or in lumbar spinal cord of mSOD1 mice by chronically inhibiting the P2X7 with the antagonist A-804598 (4, 11, 28, 43).

Given that the denervation atrophy of skeletal muscles is an early event in ALS pathology, and having established a time-dependent role exerted by P2X7 in ALS, in this work, we investigated the effects produced by the activation of this receptor in the muscular tissue of mSOD1 mice. In particular, we evaluated whether an *in vivo* treatment with BzATP just before the onset of symptoms could modify the pathological neuromuscular phenotype of mSOD1 mice.

We demonstrated that the activation of P2X7 improves the metabolism of muscle myofibers and preserves the morphology of NMJs, thus ameliorating the denervation atrophy of skeletal muscles in ALS mice.

## MATERIALS AND METHODS

### Reagents

2′-(3′)-O-(4-benzoyl-benzoyl) adenosine 5′-triphosphate triethylammonium salt (BzATP) and all other reagents, unless otherwise stated, were obtained from Sigma Aldrich (Milan, Italy).

### Mice

All animal procedures have been performed according to the European Guidelines for the use of animals in research (86/609/CEE) and the requirements of Italian laws (D.L. 26/2014). The ethical procedure has been approved by the Animal Welfare Office, Department of Public Health and Veterinary, Nutrition and Food Safety, General Management of Animal Care and Veterinary Drugs of the Italian Ministry of Health (protocol number 319/2015PR). All efforts were made to minimize animal suffering and use the minimum number of animals necessary to obtain reliable results. Adult B6.Cg-Tg(mSOD1)1Gur/J mice were obtained from Jackson Laboratories (Bar Harbor, ME, USA), bred in our indoor animal facility and genotyped as described (2). mSOD1 mice at 105 days of age [late pre-onset (3)] were randomly grouped and subjected to intraperitoneal injection of vehicle (PBS) or P2X7 specific agonist BzATP at 1 mg/kg for seven days.

### Western blotting

Protein lysates were obtained by homogenization of mice *tibialis anterior* (TA) muscles and sciatic nerves in homogenization buffer as previously described (26). Analysis of protein components (15 μg for tissue extracts) was performed by Mini-PROTEAN® TGX™ Gels (BioRad, USA) and transfer onto nitrocellulose membranes (Amersham Biosciences, USA). After saturation with blocking agent, blots were incubated overnight at 4°C with the specified antibody against anti-P2X7, rabbit (1:500 Alomone); anti-Pax7, mouse (1:100 HDB); anti-MyoG, mouse (1:10 HDB); anti-GYS, rabbit and anti-pGYS, rabbit (1:1000 Cell Signaling). Primary antibodies were then detected with HRP-conjugated secondary antibodies and visualized using ECL Advance Western blot detection kit (Amersham Biosciences, USA). Signal intensity quantification was performed by Kodak Image Station analysis software.

### Muscle denervation and neuromuscular junction morphology

TA muscles were dissected out and snap-frozen in liquid nitrogen. Serial longitudinal cryosections (20 μm) were collected on poly-lysine objective slides (VWR International). Six serial sections per animal were analyzed. Muscle sections were stained with anti-synaptic vesicle protein (SV2; 1:100 Developmental Studies Hybridoma Bank) and mouse anti-neurofilaments (2H3 1:50 Developmental Studies Hybridoma Bank). α-bungarotoxin coupled to Alexa Fluor 488 (1:500 Invitrogen) was then added and left for 1 h at room temperature. Images were obtained with an Olympus virtual slide system VS110 (Olympus, Center Valley, USA) at 20×-magnification. The colocalization channel between neurofilament and BTX immunostaining was produced for each Z-stack. The percentage of neuromuscular innervation was quantified in OlyVIA based on the overlap between neurofilaments (SV2/2H3) staining and a-BTX labeled endplates.

NMJ morphology was evaluated using the "NMJ-morph" workflow in Fiji (Image J, U.S. National Institute of Health, Bethesda, Maryland, USA) as previously described (15).

The images of α-BTX$^+$ endplates were acquired under a sequential scanning mode on an Olympus confocal scan unit FV500 (Olympus, Center Valley, USA) with the following parameters: 8 bit depth, 512 × 512 frame size, ×60 magnification, ×2.5 zoom and 1 μm *Z*-stack interval.

## Morphometric analysis of muscles

TA muscles were dissected out and snap-frozen in liquid nitrogen. Serial transverse cryosections (10 μm) were air-dried, fixed in 4% paraformaldehyde solution for 5′, and stained with Wheat Germ Agglutinin, Alexa Fluor™ 488 Conjugate (1:500; Thermo Fisher) and Hoechst (1:1000; Roche).

For the muscle composition, serial transverse cryosections (10 μm) were air-dried and then incubated at 37°C for 30′ in phosphate buffer (0.2 M, pH 7.6) containing 13.5 mg/mL Na-succinate (Sigma-Aldrich, St. Louis, MO, USA) and 0.5 mg/mL of nitro blue tetrazolium (Sigma-Aldrich, 0.29 mg/mL of buffer solution). After staining, sections were fixed with 4% paraformaldehyde, dehydrated in 15% alcohol for 5′ and finally mounted with DPX compound (Sigma Aldrich).

Images were acquired with an Olympus virtual slide system VS110 (Olympus, Center Valley, USA) at 20×-magnification and analyzed through Fiji (Image J, U.S. National Institute of Health, Bethesda, Maryland, USA) on three serial sections per animal.

## Isolation and bioenergetic analysis of isolated mitochondria

Mitochondria were isolated from the TA muscle following the isolation procedure described by Salvatori *et al* (2018). Final mitochondrial pellets for bioenergetic analysis were suspended in the Respiration Buffer (250 mM of Sucrose, 15 mM of KCl, 1 mM of EGTA, 5 mM of MgCl$_2$ and 30 mM of K$_2$HPO$_4$). Total mitochondrial concentrations were determined using the Bradford method. Mitochondria (4 μg) were loaded on the Seahorse XF96 and centrifuged for 20 minutes at 2000 × g. After centrifugation, 180 μL of respiration buffer [containing substrate: pyruvate (5 mM), malate (2.5 mM) and glutamate (5 mM)] was added to each well, and the plate was incubated at 37°C for 8 minutes to equilibrate the temperature. The XF cartridge was loaded with the following drugs: ADP, oligomycin, FCCP and antimycin A. The final concentrations of injections were 1 mM of ADP, 3 μM of oligomycin, 12 μM of FCCP and 2 μM of antimycin A. Coupling assays were performed in six replicate technical wells, repeated 3 times. XF96 data were calculated using the algorithm described and used by the Seahorse software package. Statistical analysis was conducted in PRISM (GraphPad Software) using one-way ANOVA.

## Single myofiber isolation and staining

TA, *Exstensor Digitorium Longus* and *Gastrocnemius* muscles were isolated from mice and digested for 75 minutes in 0.35% collagenase type I (Sigma, C0130)/DMEM (Gibco,

10569010) at 37°C. Three rounds of myofibers' washes were performed in pre-coated dishes with 20% FBS (Gibco, 10500064)/DMEM. Finally, the myofibers were maintained in DMEM supplemented with 20% FBS, 1% chicken embryo extract (Seralab, CE650-DL) and 1% penicillin/streptomycin (Euroclone, ECB 3001) with different concentration of BzATP (0, 10 and 100 μM) for 72 h and changing the medium every day. Myofibers were collected in 2-mL tubes pre-coated with 10% FBS/PBS and fixed for 15 minutes with 4% PFA followed by three washes in PBS. Permeabilization was performed for 8 minutes with 0.5% Triton X-100 (Sigma, 93443)/PBS followed by two washes in PBS. Myofibers were incubated for 1 h in blocking solution (10% FBS/PBS). Primary antibodies were incubated in blocking solution overnight at 4°C. The day after, the myofibers were washed twice in 0.1% FBS/PBS and incubated for 60 minutes with secondary antibodies in blocking solution. Fibers were washed in PBS, incubated for five minutes with DAPI, briefly washed twice in PBS and mounted on the slide with a drop of Prolong Antifade Pax7 (Developmental Studies Hybridoma Bank used at 1:50) MyoD (Santacruz SC-760 used at 1:100). Secondary antibodies were: Alexa 488, Jackson Immuno Research, 711-545-152 (1:200), Alexa 594, Jackson Immuno Research, 711-545-150 (1:200).

## Statistics

Data are presented as the mean ± standard error of the mean (S.E.M.). Statistical differences were verified by Student's *t*-test if the normality test was passed, or by the Mann–Whitney rank sum test, if the normality test failed, considering acceptable value for the asymmetry between −2 and +2 in order to prove normal univariate distribution. One-way analysis of variance (ANOVA) followed by post-hoc Tukey's test was used for multiple comparisons. The software package GraphPad Prism 7.03 (GraphPad Software, San Diego, CA, USA) was used for all statistical analysis with differences considered significant for $P < 0.05$.

# RESULTS

## BzATP activates the P2X7 and prevents the skeletal muscle denervation atrophy and the neuromuscular junction impairment in mSOD1 mice

To dissect some potential actions of P2X7 in peripheral muscular tissue, we first evaluated the protein levels of P2X7 in TA muscle of pre-symptomatic mSOD1 mice after BzATP treatment for one week. Although there was no difference in the P2X7 levels between WT and mSOD1 mice, BzATP treatment significantly increased the expression of the receptor compared to vehicle-treated mice (Figure 1A).

This increase correlated with a lower muscle wasting in mSOD1 mice treated with BzATP (6.2% ± 13.1) than in mice treated with vehicle (25.8% ± 10.9) (Figure 1B).
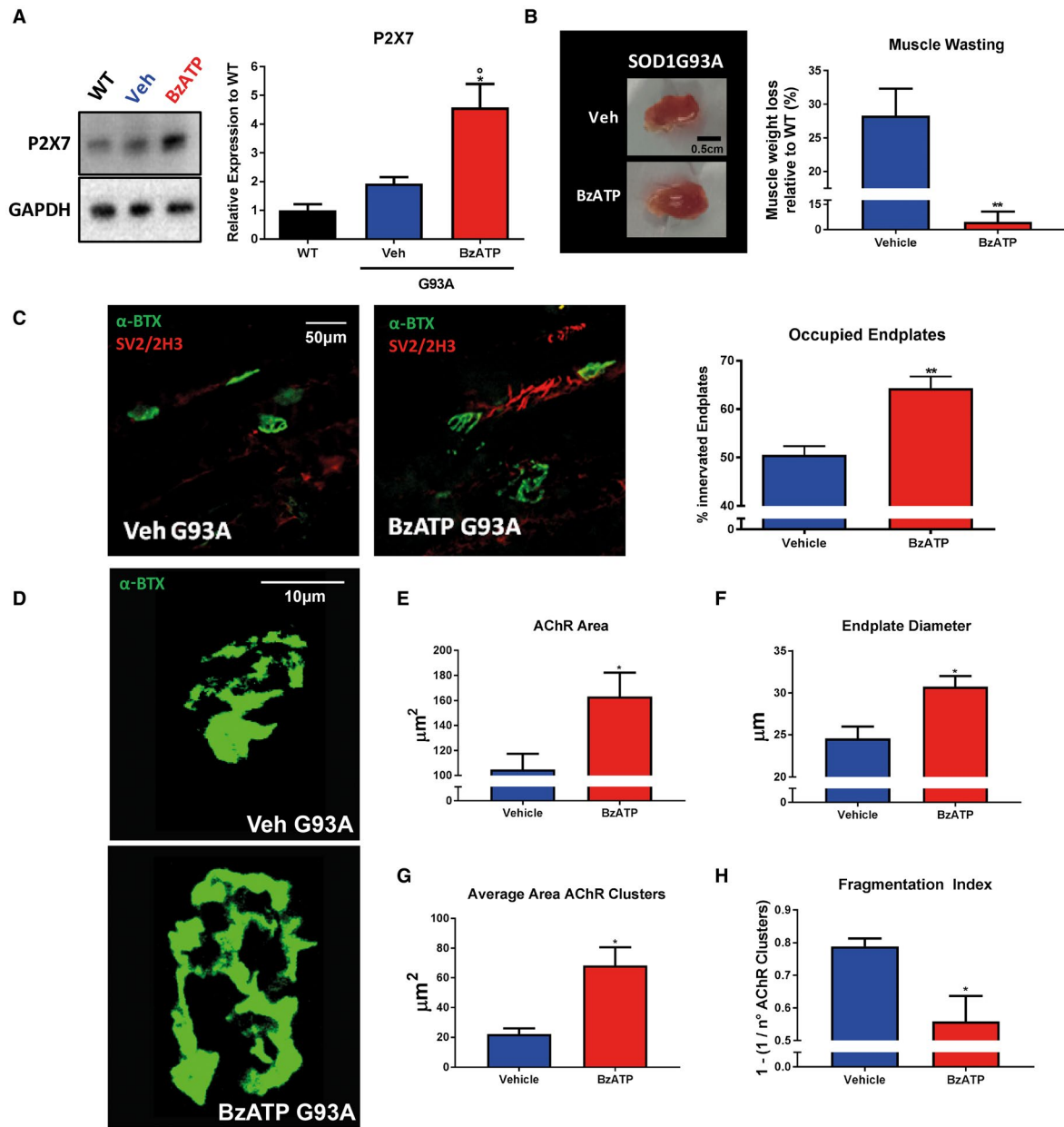
**Figure 1.** *BzATP upregulates P2X7 receptor and reduces atrophy of TA muscle in mSOD1 mice.* **A.** An equal amount of total *tibialis anterior* (TA) muscle lysates from WT mice and vehicle- or BzATP-treated mSOD1 mice at the pre-symptomatic stage (n = 4/group) were subjected to immunoblotting with anti-P2X7. GAPDH was used for protein normalization. **B.** Representative image of the TA muscle from vehicle- and BzATP-treated mSOD1 mice and relative muscle weight quantification. **C.** Analysis of denervation on TA muscle of vehicle- and BzATP-treated mSOD1 mice is calculated by the percentage of occupied endplates. Data represent means ± SEM. Statistical significance was calculated by one-way ANOVA with Tukey's post-analysis or Student's *t*-test, as referred to WT, °$P < 0.05$ or to vehicle mice *$P < 0.05$; **$P < 0.01$. **D.** Representative confocal images of the endplates of vehicle and BzATP-treated mice. **E.** AChR area, **F.** endplate diameter, **G.** average AChR Area and **D.** the fragmentation index were measured on ~no. 15 randomly selected α-BTX⁺ endplates for each animal. Data represent means ± SEM. Statistical significance was calculated by Student's *t*-test. *$P < 0.05$.

Consistently, the denervation of TA muscles was lower in mSOD1 mice treated with BzATP compared to the vehicle-treated group, as evinced by significant preservation of innervated endplates (Figure 1C).

Given that P2X7 is the only purinergic receptor at the NMJ (9), we evaluated if the activation of the receptor could be involved in the preservation of NMJ integrity.

We found that BzATP-treated animals had NMJs with a higher AChR area (BzATP: 163.2 ± 37 μm$^2$; Vehicle: 104.7 ± 25 μm$^2$), and endplate diameter (BzATP: 30.7 ± 2.5 μm; Vehicle: 24.5 ± 2.8 μm), and a reduced fragmentation index (BzATP: 0.55 ± 0.15; Vehicle: 0.78 ± 0.04) than the controls.

## BzATP restores a glycolytic phenotype in *tibialis anterior* muscle fibers of mSOD1 mice

It has been previously demonstrated that during ALS disease there is a progressive shift in the skeletal muscle fibers from a rapid contraction to a slow contraction phenotype, which would result in a shift toward an increased oxidative metabolism (44). To study the potential involvement of P2X7 in this metabolic switch, we assessed the oxidative TA muscle fiber composition after BzATP treatment in mSOD1 mice, by using the succinic dehydrogenase (SDH) histochemical assay. As shown in Figure 2A, the oxidative fibers accounted for 37% (±1.7) of total muscle fibers in WT mice, whereas in mSOD1 mice they accounted for about 57% (±1.5). BzATP maintained the number of oxidative fibers in mSOD1 mice at the levels observed in the WT group (35% ± 3.8) (Figure 2A). To evaluate if the glycolytic-oxidative fiber switching was correlated with a difference in the rate of glucose uptake/storage, we next investigated the levels of the glycogen synthase (Gys) inhibition, by assessing the extent of its phosphorylation. We found that the phosphorylation of Gys (pGys) was remarkably increased in mSOD1 mice treated with BzATP compared to mice treated with vehicle, where the increase was not statistically significant to WT mice (Figure 2B). This would suggest that activation of P2X7 signaling in muscle fibers inhibits glycogen synthesis in favor of glucose consumption.

## BzATP improves the mitochondrial respiration in *tibialis anterior* muscle of mSOD1 mice

The switch from glycolytic to high oxidative metabolism that occurs in the early stages of the pathology (44) is associated with a concomitant mitochondrial dysfunction in ALS muscle (32).

We, therefore, asked whether P2X7 activation was able to modulate mitochondrial activity and ATP synthesis. To this aim, we performed a coupling mitochondrial assay on isolated mitochondria obtained from TA muscle of mSOD1 mice and their WT littermates, after BzATP treatment for one week. By tracing O$_2$ consumption rates (OCR), this assay allows evaluating the flow of oxidative phosphorylation and the electron transport chain functionality. As shown in Figure 2C, OCR was measured under baseline conditions (State 2), and in response to administration of ADP (State 3, coupled maximal respiration), then Oligomycin A (State 4o, residual respiration caused by proton leak), then FCCP (State 3u, uncoupled maximal respiration) and finally Antimycin A (IOR, inhibition of oxidative respiration).

In TA of mSOD1 compared with WT mice, we observed a marked impairment of all mitochondrial functionalities, but BzATP treatment partially recovered OCR (Figure 2C–D). Of note, BzATP induced a significant increase of the maximal coupled respiration, State 3, thus indicating a recovery in ATP production (Figure 2D). Finally, respiratory control ratio (RCR), obtained by dividing State 3 by State 4o and representative of mitochondrial efficiency, confirmed that BzATP treatment can restore, albeit partially, mitochondria coupling efficiency (Figure 2E).

## BzATP increases the differentiation of skeletal muscle satellite cells in mSOD1 mice

To investigate whether the reduction of muscular atrophy observed after BzATP treatment could reflect a functional improvement of mSOD1 muscle, we next assessed by western blot the expression levels of two key myogenic transcription factors: Pax7, the hallmark of muscle stem cell (SCs) (22) and MyoG, a marker of early commitment and muscle differentiation (13, 46). BzATP treatment stimulated the expression of both Pax7 (Figure 3A) and MyoG (Figure 3B), suggesting an improved proliferation of SCs and myogenic differentiation. Moreover, BzATP treatment in mSOD1 mice determined an increase of centro-nucleated myofibers (Figure 3C) which are the sign of newborn myofibers, suggesting an amelioration of the muscle regeneration (48). These data further support the beneficial effect of BzATP on myogenesis and suggest that BzATP directly influences muscle regeneration signaling in mSOD1 TA muscle.

## BzATP enhances the proliferative capacity of Satellite Cells

Muscle regeneration and growth is mostly regulated by SCs, the muscle stem cells characterized by the expression of the Pax7 transcriptional factor. SCs support the muscle homeostasis through their capacity to activate and to start differentiation and self-renewal. A crucial transcriptional factor that drives these processes is MyoD, which regulates the transition of SCs from the state of quiescence toward the activation (1, 51). To dissect the effect of BzATP on SCs, we isolated single myofibers from WT and mSOD1 mice. Upon 72 h in growing medium, each SC associated to myofibers formed a cluster of cells composed by activated (Pax7+/MyoD+), differentiating (Pax7-/MyoD+) and self-renewal (Pax7+/MyoD-) cells (51) (Figure 3D).

We found that mSOD1 SCs show an impaired proliferation within the cluster (Dapi$^+$ cells) compared to WT (Figure 4E). Administration of BzATP (100 μM) to single-cultured myofibers induced a recovery of the total number of cells within the cluster (Figure 3E) and of SCs (Pax7+) (Figure 4F). In addition, while untreated mSOD1 mice showed no difference in the number of activated (Pax7+/MyoD+) and self-renewing (Pax7+/MyoD−) SCs compared to WT, they exhibited defects in muscle differentiation as
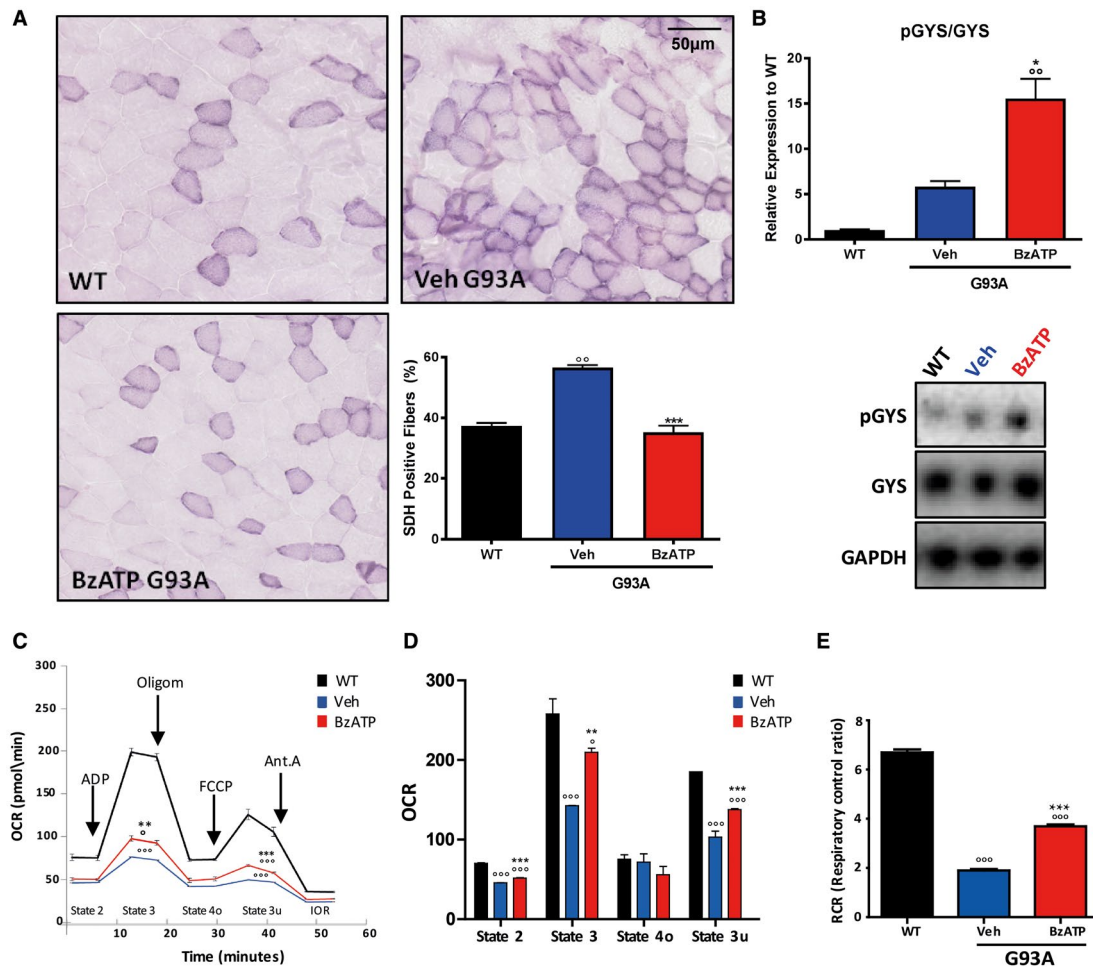
**Figure 2.** *BzATP induces a glycolytic phenotype and improves mitochondrial respiration in TA muscles of mSOD1 mice.* **A.** Transverse muscle sections from WT and mSOD1 mice at the pre-symptomatic stage were stained for SDH in order to identify oxidative muscle fibers. **B.** An equal amount of total *tibialis anterior* (TA) muscle lysates from WT and vehicle- or BzATP-treated mSOD1 mice at the pre-symptomatic stage (n = 4/group) were subjected to western blotting with anti-pGYS and GYS. GAPDH was used for protein normalization. **C.** A representative coupling assay using isolated mitochondria and OCR response to ADP, oligomycin, FCCP and Antimycin A. **D.** The histogram represents baseline conditions, or State 2, maximal coupled respiration, or State 3, respiration caused by proton leak, or State 4o, maximal uncoupled respiration, or State 3u. **E.** The histogram represents respiratory control ratio (RCR) in mSOD1 mice treated with BzATP, vehicle and in WT mice. Data represent means ± SEM. Statistical significance was calculated by one-way ANOVA with Tukey's post-analysis or Student's *t*-test, as referred to WT, $°P < 0.05$; $°°P < 0.01$; $°°°P < 0.001$ or to vehicle mice $*P < 0.05$; $**P < 0.01$; $***P < 0.001$.

shown by the lower number of Pax7−/MyoD+ SCs (Figure 3G). Remarkably, BzATP treatment (100 µM) ameliorated this defect. All together, these data confirm that BzATP treatment improves proliferation and differentiation of muscle stem cells.

## DISCUSSION

Specific P2X7 signaling events trigger a host of cellular responses dramatically varying from increased survival/growth to apoptosis/necrosis and cell death (49). However, the functional importance of P2X7 receptors in skeletal muscles is still unclear and the effects appear to be complex.

The general finding of upregulated expression and function of P2X7 in dystrophic myoblasts (14) suggest that they may have shared roles in several different pathologies. P2X7 receptors are classically coupled to extracellular ATP-induced cell death and the release of immune/inflammatory modulators (38). This might be of particular relevance in skeletal muscle, where degenerating fibers provide potential sources of extracellular ATP at concentrations exceeding those that can be reached anywhere else in the body (49). Nevertheless, it is also well recognized that in developing and regenerating muscles, extracellular ATP acting through tightly regulated P2X and P2Y receptors has beneficial roles in myogenesis, SC/myoblast proliferation, motility and differentiation (21).
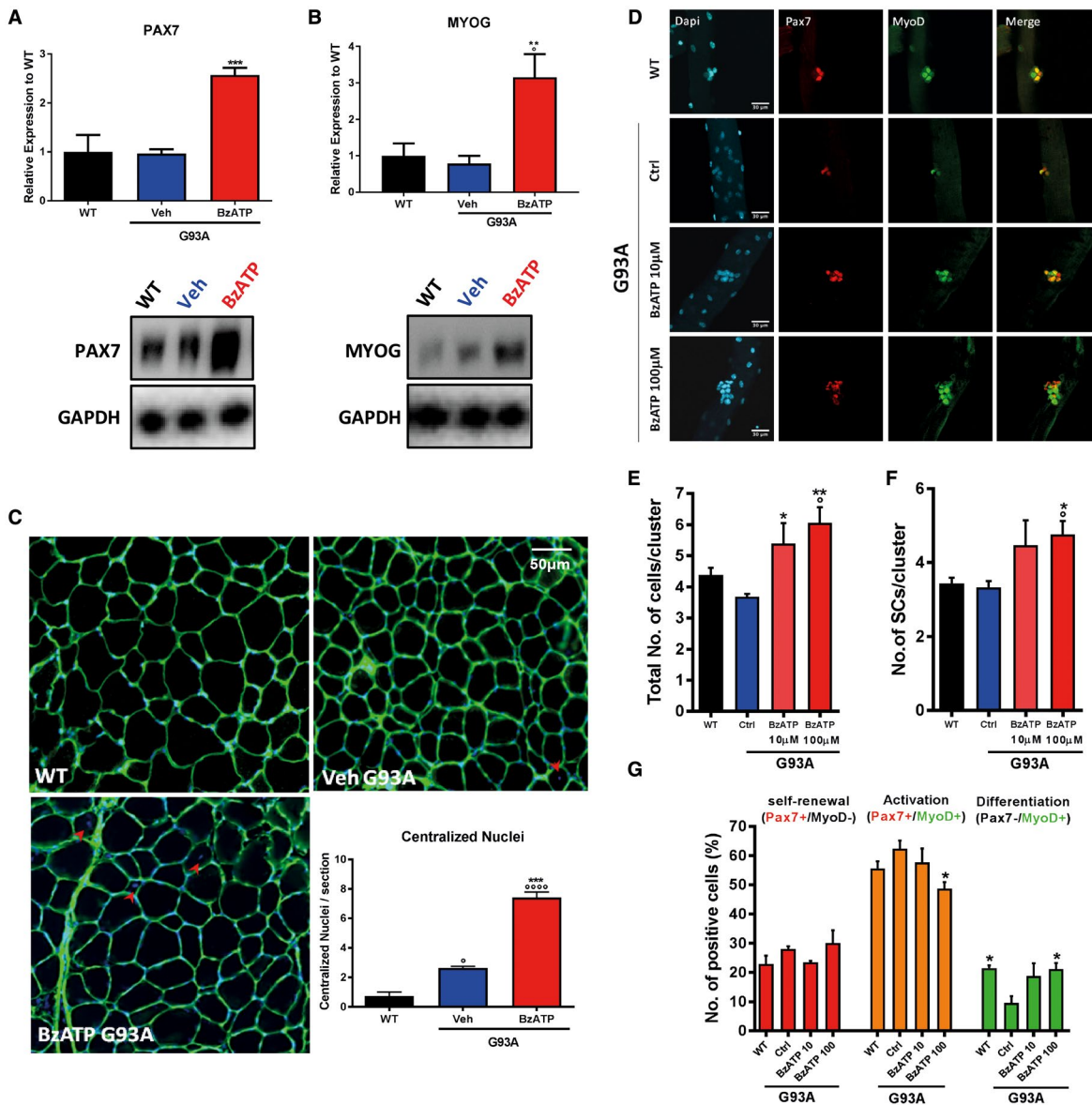
**Figure 3.** *BzATP enhances the activation of myogenic satellite cells in skeletal muscles of mSOD1 mice.* An equal amount of total *tibialis anterior* (TA) muscle lysates from WT and vehicle- or BzATP-treated mSOD1 mice at pre-symptomatic stage (n = 4/group) were subjected to western blotting with **A.** anti-PAX7 and **B.** anti-MYOG. GAPDH was used for protein normalization. **C.** Transverse muscle sections from mSOD1 mice at the 112 days were histochemically stained for the count of centralized nuclei (indicated with red arrows). Data represent means ± SEM. Statistical significance was calculated by one-way ANOVA with Tukey's post-analysis or Student's *t*-test, as referred to WT, °$P$ < 0.05; °°$P$ < 0.01; °°°$P$ < 0.001; °°°°$P$ < 0.0001 or to vehicle mice *$P$ < 0.05; **$P$ < 0.01; ***$P$ < 0.001. **D.** Myofibers from WT and mSOD1 mice treated with vehicle, BzATP 10 mM and BzATP 100 mM were stained (after 72 h in culture) with anti-Pax7 and anti-MyoD. DAPI was used to identify all myofibers nuclei. The graphs represent the quantification of the total number of cells/cluster (**E**), the number of SCs/cluster (**F**) and the distribution of self-renewing (in red, Pax7+/MyoD-), activated (in yellow, Pax7+/MyoD+) and differentiating cells (in green, Pax7-/MyoD+) in myofibers (**G**). Data represent means ± SEM. Statistical significance was calculated by one-way ANOVA with Tukey's post-analysis or Student's *t*-test, as referred to WT fibers, °$P$ < 0.05; or to ctrl G93A fibers, *$P$ < 0.05; **$P$ < 0.01.

In ALS, the increased purinergic signaling occurring in microglia and motor neurons of mSOD1 mice and rats has been always considered to contribute to the development and maintenance of the inflammatory response (42). However, clear evidence indicates that P2X7 may have a dual function in the onset and progression of ALS, either trophic and anti-inflammatory, or toxic and pro-inflammatory. In detail, we have previously shown that the genetic ablation of P2X7 in mSOD1 mice anticipates the disease onset and exacerbates the disease progression (2). On the
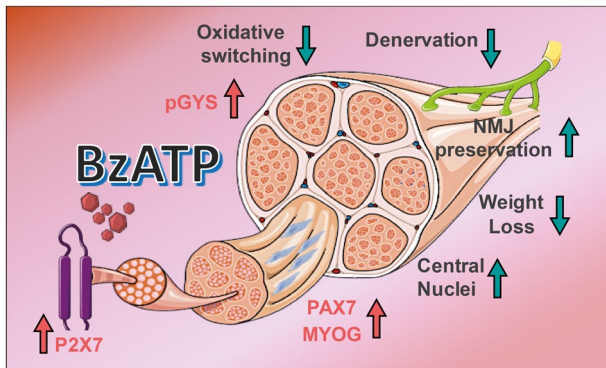
**Figure 4.** *BzATP administration counteracts the denervation atrophy of hind limb skeletal muscles of mSOD1 mice.* Schematic representation of the effects produced by BzATP administration on the *tibialis anterior* muscle of mSOD1 mice.

contrary, the systemic pharmacological antagonism of P2X7 gives positive outcomes but limited to a definite late stage of disease progression (3). These results thus suggest a twofold role of P2X7 in the course of the disease, so that the involvement of P2X7 in ALS might not be univocal, and affect different molecular and systemic levels.

To disentangle this issue, in the present study, we went beyond the CNS by analyzing the P2X7 signaling in the hind limb skeletal muscles of mSOD1 mice. We found that the induction of P2X7 through its most specific agonist, BzATP, at the late pre-onset stage significantly delays muscle denervation and muscle atrophy (26), which are early hallmarks of disease progression in mSOD1 mice.

## BzATP restores the glycolytic energy demand and counteracts the mitochondrial dysfunction in skeletal muscles of mSOD1 mice

The overexpression of mSOD1 in skeletal muscles of mice induces a metabolic switch toward lipid use in glycolytic myofibers (44). This early pathological event in ALS mouse models is also accompanied by mitochondrial impairment. For instance, the accumulation of mSOD1 in the mitochondria skeletal muscles is causally linked to the depolarization of mitochondrial membrane potential and abnormal mitochondrial dynamics (20). Interestingly, the presence of aggregates of mitochondria in the subsarcolemmal region of skeletal muscles and the increased mitochondria volume and morphological alterations are reported in muscle biopsies in ALS (12, 18, 19, 25, 37). Moreover, mitochondrial metabolic dysfunctions such as decreased oxidative capacity and alteration in $Ca^{2+}$ handling have been described in skeletal muscle of ALS animal models and patients (19). Noteworthy, the restoration of the metabolic equilibrium in glycolytic muscle fibers of ALS mice following dichloride acetate treatment is able to protect muscle mitochondria and prevent oxidative stress, while also ameliorating denervation and atrophy (10, 44).

Here we found that BzATP administration induces a significant increase in P2X7 levels and a pronounced phosphorylation of the glycogen synthase in muscle fibers. Accordingly, the activation of the P2X7 signaling inhibits the glycogen synthesis and possibly increases the free glucose availability. In keeping with this, Kim *et al* (2012) reported that extracellular ATP through P2 receptors positively influences the rate of glucose uptake in C2C12 myotubes by facilitating the translocation of GLUT1 and GLUT4 glucose transporters into the plasma membrane (35). This suggests that BzATP-mediated stimulation of muscular P2X7 during the disease course of mSOD1 mice may have contributed to increasing glucose availability and transport, thus supporting the energy demand of glycolytic myofibers. Sustaining this hypothesis, the glycolytic vs. oxidative muscle fiber composition of the TA muscles in mSOD1 mice is increased by P2X7 activation, being BzATP able to restore the percentage of fast fatigable muscle fibers to levels comparable to WT mice. Moreover, the restoration of glycolytic metabolism in BzATP-treated mSOD1 mice partially preserves the mitochondrial metabolism and ATP production in myofibers.

Finally, BzATP may directly influence mitochondrial respiration through P2X7-dependent calcium influx. In support of this, Juaristi *et al* (2018) showed that extracellular ATP produces a substantial stimulation of respiration in primary culture of astrocytes, caused by a $Ca^{2+}$-dependent upregulation of cytosolic pyruvate production. Interestingly, astrocytes are glycolytic cells (16), where an increased ATP demand produced by different workloads is met by increased glycolysis, but also by mitochondrial oxidative phosphorylation (36). In response to extracellular ATP, astrocytes upregulate glycolysis and lactate production, but also pyruvate production and utilization in mitochondria, by respiration (16). This scenario closely resembles the composite organization of skeletal muscles, where fast fatigable glycolytic myofibers coexist with slow resistant oxidative myofibers. Our results clearly confirm the double role of BzATP also in boosting the overall mSOD1 muscle metabolism, to face the increased energy demand of both myofiber types during ALS disease progression.

## BzATP improves the differentiation of myogenic satellite cells in skeletal muscles of mSOD1 mice

In addition to a positive activity toward myofibers metabolism, we also found that the stimulation of P2X7 with BzATP increases the activation and differentiation of satellite cells in skeletal muscles of mSOD1 mice. This evidence is strengthened *ex vivo* by observing that BzATP administration to mSOD1 myofibers increases the expansion of SC progeny on single myofibers and the percentage of differentiated Pax7⁻-MyoD⁺ cells. Our results thus support a previous observation showing the P2X7-dependent proliferation of C2C12 mouse myoblasts (21).

Overall, these findings suggest that in dysfunctional or damaged skeletal muscles, extracellular ATP may work as an autocrine signal for myofibers, essential to promote muscle regeneration through the stimulation of the P2X7 pathway.

## CONCLUSIONS

In processes related to CNS injury, nucleotide receptor activity accounts for changes and adaptations in different cell populations. In these conditions, purinergic receptors, particularly the P2X7 ionotropic subtype, act as primary sensors of extracellular ATP (40). The increased purinergic signaling that follows CNS impairment has been always considered to contribute to the development and maintenance of the subsequent inflammatory response (34). Therefore, it is not surprising that the design of new purinergic ligands with therapeutic potential is usually based on antagonistic action on P2X receptors (6). Nevertheless, many examples of protective and trophic actions of purinergic agonists are emerging, adding new clues to the role of these receptors in animal models of neurodegenerative diseases, ischemic stroke and spinal cord injury. Moreover, purinergic receptors also play an active role in neurogenesis (30). This implies that special caution has to be taken when using drugs or pharmacological tools that systematically block these receptors. In fact, whether nucleotide receptor activation is beneficial or detrimental depends on different factors, including the nature and the duration of the toxic insult, and the specific target cell population, both converging in a precise temporal window of the injury event.

P2X7 is the only purinergic receptor expressed at the NMJs and its activation through BzATP modulates vesicle release at the mouse motor nerve terminals (9, 23, 24, 45). However, the functional effects of this activation have never been investigated. Our study clearly shows that the activation of P2X7 signaling in mSOD1 mice at a late pre-symptomatic stage preserves the morphology of NMJs. Moreover, P2X7 activation is twofold effective in the skeletal muscle metabolism, by enhancing the glycolytic fiber metabolism and by supporting the mitochondrial respiration. At the same time, we found that the induction of P2X7 promotes myogenic SCs activation/differentiation. All together, these effects delay the denervation atrophy of hind limb skeletal muscles of mSOD1 mice (Figure 4).

The role of P2X7 signaling in ALS skeletal muscle is a novel issue extending our previous evidence about the multisystem function of this receptor in ALS. Although we demonstrated that by boosting the P2X7 axis during the pre-onset stages we can counteract the muscle denervation atrophy in the periphery of mSOD1 mice, further analysis will be necessary to investigate the effect of a prolonged or later administration of BzATP on the disease course of ALS mouse models.

Despite many lines of evidence provided for the essential contribution of the P2X7 signaling to the motor neuron damage and microgliosis, it is important to emphasize that in the therapy of ALS there are currently no clinical trials targeting the purinergic players. Given the complexity of the purinome (39, 43), further intense research still has to be done to elucidate the various implications of the purinergic signaling in ALS, and to evaluate its therapeutic potential. In the present report, we have provided clear evidence that a P2X7-targeted and site-specific modulation might be an additional strategy to interfere with the complex multifactorial and multisystem nature of ALS.

## AUTHOR CONTRIBUTIONS

Study concept and design: PF, SA, CB, GN and CVo. Data acquisition and analysis: PF, SA, AB, IS, CVa, CL, CB, GN and CVo. Manuscript writing: PF, SA, GN and CVo. All authors edited and approved the final version of the manuscript.

## CONFLICTS OF INTEREST

The authors have no competing financial interests to disclose.

## DATA AVAILABILITY STATEMENT

Data, materials and software information supporting the conclusions of this article are included within the article.

## REFERENCES

1. Almada AE, Wagers AJ (2016) Molecular circuitry of stem cell fate in skeletal muscle regeneration, ageing and disease. *Nat Rev Mol Cell Biol* **17**:267–279.
2. Apolloni S, Amadio S, Montilli C, Volonte C, D'Ambrosi N (2013) Ablation of P2X7 receptor exacerbates gliosis and motoneuron death in the SOD1-G93A mouse model of amyotrophic lateral sclerosis. *Hum Mol Genet* **22**:4102–4116.
3. Apolloni S, Amadio S, Parisi C, Matteucci A, Potenza RL, Armida M *et al* (2014) Spinal cord pathology is ameliorated by P2X7 antagonism in a SOD1-mutant mouse model of amyotrophic lateral sclerosis. *Dis Model Mech* **7**:1101–1109.
4. Apolloni S, Parisi C, Pesaresi MG, Rossi S, Carri MT, Cozzolino M *et al* (2013) The NADPH oxidase pathway is dysregulated by the P2X7 receptor in the SOD1-G93A microglia model of amyotrophic lateral sclerosis. *J Immunol* **190**:5187–5195.
5. Bartlett R, Sluyter V, Watson D, Sluyter R, Yerbury JJ (2017) P2X7 antagonism using Brilliant Blue G reduces body weight loss and prolongs survival in female SOD1 G93A amyotrophic lateral sclerosis mice. *PeerJ* **5**:e3064.
6. Burnstock G (2017) Purinergic signalling: therapeutic developments. *Front Pharmacol* **8**:661.
7. Campanari M-L, García-Ayllón M-S, Ciura S, Sáez-Valero J, Kabashi E (2016) Neuromuscular junction impairment in

amyotrophic lateral sclerosis: reassessing the role of acetylcholinesterase. *Front Mol Neurosci* **9**:160.

8. Chen S, Sayana P, Zhang X, Le W (2013) Genetics of amyotrophic lateral sclerosis: an update. *Mol Neurodegener* **13**:8–28.

9. Deuchars SA, Atkinson L, Brooke RE, Musa H, Milligan CJ, Batten TFC *et al* (2001) Neuronal P2X 7 receptors are targeted to presynaptic terminals in the central and peripheral nervous systems. *J Neurosci* **21**:7143–7152.

10. Dobrowolny G, Lepore E, Martini M, Barberi L, Nunn A, Scicchitano BM, Musarò A (2018) Metabolic changes associated with muscle expression of SOD1G93A. *Front Physiol* **9**:1–9.

11. Fabbrizio P, Amadio S, Apolloni S, Volonté C (2017) P2X7 receptor activation modulates autophagy in SOD1-G93A mouse microglia. *Front Cell Neurosci* **11**:249.

12. Ferri A, Coccurello R (2017) What is "hyper" in the ALS hypermetabolism? *Mediators Inflamm* **2017**:1–11.

13. Francetic T, Li Q (2011) Skeletal myogenesis and Myf5 activation. *Transcription* **2**:109–114.

14. Górecki DC (2019) P2X7 purinoceptor as a therapeutic target in muscular dystrophies. *Curr Opin Pharmacol* **47**:40–45.

15. Jones RA, Reich CD, Dissanayake KN, Kristmundsdottir F, Findlater GS, Ribchester RR *et al* (2016) NMJ-morph reveals principal components of synaptic morphology influencing structure—function relationships at the neuromuscular junction. *Open Biol* **6**:160240.

16. Juaristi I, Llorente-Folch I, Satrústegui J, del Arco A (2019) Extracellular ATP and glutamate drive pyruvate production and energy demand to regulate mitochondrial respiration in astrocytes. *Glia* **67**:759–774.

17. Kovanda A, Leonardis L, Zidar J, Koritnik B, Dolenc-Groselj L, Ristic Kovacic S *et al* (2018) Differential expression of microRNAs and other small RNAs in muscle tissue of patients with ALS and healthy age-matched controls. *Sci Rep* **8**:5609.

18. Krasnianski A, Deschauer M, Neudecker S, Gellerich FN, Müller T, Schoser BG *et al* (2005) Mitochondrial changes in skeletal muscle in amyotrophic lateral sclerosis and other neurogenic atrophies. *Brain* **128**:1870–1876.

19. Loeffler JP, Picchiarelli G, Dupuis L, Gonzalez De Aguilar JL (2016) The role of skeletal muscle in amyotrophic lateral sclerosis. *Brain Pathol* **26**:227–236.

20. Luo G, Yi J, Ma C, Xiao Y, Yi F, Yu T, Zhou J (2013) Defective mitochondrial dynamics is an early event in skeletal muscle of an amyotrophic lateral sclerosis mouse model. *PLoS One* **8**:e82112.

21. Martinello T, Baldoin MC, Morbiato L, Paganin M, Tarricone E, Schiavo G *et al* (2011) Extracellular ATP signaling during differentiation of C2C12 skeletal muscle cells: role in proliferation. *Mol Cell Biochem* **351**:183–196.

22. Mauro A (1961) Satellite cell of skeletal muscle fibers. *J Cell Biol* **9**:493–495.

23. Miteva AS, Gaydukov AE, Shestopalov VI, Balezina OP (2018) Mechanism of P2X7 receptor-dependent enhancement of neuromuscular transmission in pannexin 1 knockout mice. *Purinergic Signal* **14**:459–469.

24. Moores TS, Hasdemir B, Deuchars J, Parson SH (2005) Properties of presynaptic P2X 7 -like receptors at the neuromuscular junction. *Brain Res* **1034**:40–50.

25. Myoung JC, Suh YL (2002) Ultrastructural changes of mitochondria in the skeletal muscle of patients with amyotrophic lateral sclerosis. *Ultrastruct Pathol* **26**:3–7.

26. Nardo G, Trolese MC, Verderio M, Mariani A, de Paola M, Riva N *et al* (2018) Counteracting roles of MHCI and CD8+ T cells in the peripheral and central nervous system of ALS SOD1G93A mice. *Mol Neurodegener* **13**:42.

27. Nijssen J, Comley LH, Hedlund E (2017) Motor neuron vulnerability and resistance in amyotrophic lateral sclerosis. *Acta Neuropathol* **133**:863–885.

28. Parisi C, Arisi I, D'Ambrosi N, Storti AE, Brandi R, D'Onofrio M, Volonté C (2013) Dysregulated microRNAs in amyotrophic lateral sclerosis microglia modulate genes linked to neuroinflammation. *Cell Death Dis* **4**:e959.

29. Philips T, Rothstein JD (2015) Rodent models of amyotrophic lateral sclerosis. *Curr Protoc Pharmacol* **69**:5.67.1–5.67.21.

30. Rodrigues RJ, Marques JM, Cunha RA (2018) Purinergic signalling and brain development. *Semin Cell Dev Biol* pii: S1084-9521(18)30065-X.

31. Scaramozza A, Marchese V, Papa V, Salaroli R, Sorarù G, Angelini C, Cenacchi G (2014) Skeletal muscle satellite cells in amyotrophic lateral sclerosis. *Ultrastruct Pathol* **38**:295–302.

32. Smith EF, Shaw PJ, De Vos KJ (2017) The role of mitochondria in amyotrophic lateral sclerosis. *Neurosci Lett* pii: S0304-3940(17)30544-X.

33. Song X, Xu X, Zhu J, Guo Z, Li J, He C *et al* (2015) Up-regulation of P2X7 receptors mediating proliferation of Schwann cells after sciatic nerve injury. *Purinergic Signal* **11**:203–213.

34. Sperlágh B, Illes P (2014) P2X7 receptor: an emerging target in central nervous system diseases. *Trends Pharmacol Sci* **35**:537–543.

35. Suk Kim M, Lee J, Ha J, Soo Kim S, Kong Y, Ho Cho Y *et al* (2002) ATP stimulates glucose transport through activation of P2 purinergic receptors in C2C12 skeletal muscle cells. *Arch Biochem Biophys* **401**:205–214.

36. Tarasov AI, Griffiths EJ, Rutter GA (2012) Regulation of ATP production by mitochondrial $Ca^{2+}$. *Cell Calcium* **52**:28–35.

37. Tsitkanou S, Gatta PAD, Russell AP (2016) Skeletal muscle satellite cells, mitochondria, and MicroRNAs: their involvement in the pathogenesis of ALS. *Front Physiol* **7**:403.

38. Di Virgilio F, Dal Ben D, Sarti AC, Giuliani AL, Falzoni S (2017) The P2X7 receptor in Infection and Inflammation. *Immunity* **47**:15–31.

39. Volonté C, Amadio S, D'Ambrosi N, Colpi M, Burnstock G (2006) P2 receptor web: complexity and fine-tuning. *Pharmacol Ther* **112**:264–280.

40. Volonte C, Apolloni S, D. Skaper S, Burnstock G, (2012) P2X7 Receptors: Channels, Pores and More. *CNS Neurol Disord - Drug Targets* **11**(6):705–721.

41. Volonte C, Apolloni S, Parisi C (2015) MicroRNAs: newcomers into the ALS picture. *CNS Neurol Disord - Drug Targets* **14**:194–207.

42. Volonté C, Apolloni S, Parisi C, Amadio S (2016) Purinergic contribution to amyotrophic lateral sclerosis. *Neuropharmacology* **104**:180–193.

43. Volonté C, D'Ambrosi N (2009) Membrane compartments and purinergic signalling: the purinome, a complex interplay among ligands, degrading enzymes, receptors and transporters. *FEBS J* **276**:318–329.

44. Volonté C, Parisi C, Apolloni S (2015) New kid on the block: does histamine get along with inflammation in amyotrophic lateral sclerosis? *CNS Neurol Disord Drug Targets* **14**:677–686.

45. De Vos KJ, Hafezparast M (2017) Neurobiology of axonal transport defects in motor neuron diseases: opportunities for translational research? *Neurobiol Dis* **105**:283–299.

46. Wang Y, Jaenisch R (1997) Myogenin can substitute for Myf5 in promoting myogenesis but less efficiently. *Development* **124**:2507–2513.

47. Wang Y, Jaenisch R (1997) Myogenin can substitute for Myf5 in promoting myogenesis but less efficiently. *Development* **124**:2507–2513.

48. Yin H, Price F, Rudnicki MA (2013) Satellite cells and the muscle stem cell niche. *Physiol Rev* **93**:23–67.

49. Young CNJ, Sinadinos A, Gorecki DC (2013) P2X receptor signaling in skeletal muscle health and disease. *WIREs Membr Transp Signal* **2**:265–274.

50. Young CNJ, Sinadinos A, Lefebvre A, Chan P, Arkle S, Vaudry D, Gorecki DC (2015) A novel mechanism of autophagic cell death in dystrophic muscle regulated by P2RX7 receptor large-pore formation and HSP90. *Autophagy* **11**:113–130.

51. Zammit PS, Golding JP, Nagata Y, Hudon V, Partridge TA, Beauchamp JR (2004) Muscle satellite cells adopt divergent fates. *J Cell Biol* **166**:347–357.